

# Significant local sea level variations caused by continental hydrology signals

Rebecca McGirr<sup>1,2</sup>, Paul Tregoning<sup>1,2</sup>, Anthony Purcell<sup>1</sup>, Herb McQueen<sup>1</sup>

<sup>1</sup>Research School of Earth Sciences, Australian National University, Canberra, ACT, 0200, Australia

<sup>2</sup>The Australian Centre for Excellence in Antarctic Science, University of Tasmania, Hobart, Tasmania  
7001, Australia

## Key Points:

- Exchange of water between continents and oceans causes global sea level change at rates comparable to the contributions of ice sheets
- The direct gravitational attraction effect on local sea level is of a larger magnitude than the far-field sea level changes
- Inter-annual continental hydrology signal impacts on local sea level have negated the impacts of melting polar ice sheets in some locations

## Abstract

Space gravity missions have enabled the quantification of ocean mass increase over the past two decades due to exchanges between continents and oceans. Globally, non-steric sea level rise is predominantly driven by melting polar ice sheets and mountain glaciers. However, continental hydrological processes also contribute to sea level change at significant magnitudes. We show that for most coastal areas in low-to-mid latitudes, up to half of local non-steric sea level rise is due to changes in water storage in ice-free continental regions. At other locations the direct attraction effect of anthropogenic pumping of groundwater over the duration of the GRACE and GRACE-FO mission offsets sea level rise from ice sheet and glacier melt. If these trends in continental hydrological storage were to slow or stop, these regions would experience greatly accelerated sea-level rise, posing a risk to coastal settlements and infrastructure, however, sea level rise elsewhere would be reduced.

## Plain Language Summary

It is well understood that melting of polar ice sheets and mountain glaciers cause increases in ocean mass, leading to a corresponding rise in global sea level. What is not as obvious is that multi-year changes in the storage of water on continents not covered by ice also contribute significantly to changes in global sea level. Over recent years and in some locations, the magnitude of these ‘continental hydrology’ contributions to sea level changes have been comparable to the contributions of the ice-covered regions. In some cases, the former have offset the ice sheet contributions, thus reducing regional sea level rise to substantially smaller magnitudes. Through an analysis of space gravity data, we have quantified the effects of continental hydrology on regional sea level and show that changes caused both naturally (e.g. through La Niña events) and through anthropogenic activities (e.g. extraction of groundwater) can increase or decrease regional sea level by significant amounts.

## 1 Introduction

Increases in ocean mass has risen global mean sea level at a rate of  $2.5 \pm 0.4$  mm/yr (Tapley et al., 2019); however, the most important impact of sea level variations on society lies in the local changes rather than global averages. Ocean mass variations are predominantly caused by movement of water, including mass balance change of polar ice sheets (Velicogna & Wahr, 2013; Tapley et al., 2019) (Greenland and Antarctica) and glaciated regions (Wouters et al., 2019; Ciraci et al., 2019) (e.g. Alaska, Patagonia, Svalbard), and changes in soil moisture, surface water and groundwater on continents (Leblond et al., 2009; Rodell et al., 2019). Closure of the sea level budget has been the focus of many studies (e.g. Barnoud et al., 2023) and involves the apportioning of contributions from polar ice sheets, mountain glaciers, and terrestrial water storage which are further amplified by steric expansion of the oceans as they warm. Rather than considering local sea level changes, studies of this process tend to focus on integrated sea level signals over the global oceans and use a combination of ocean height changes measured by satellite altimetry, ocean mass change from space gravity missions and temperature and salinity changes in the oceans from Argo floats (Roemmich et al., 2009) and expendable bathythermograph observations (e.g. Boyer et al. (2016)).

Exchanges of water between continents and oceans includes three additional components that directly affect ocean height beyond the simple volumetric effect. First, variations in the water mass on the continent change the direct gravitational attraction between the oceans and continents (Mitrovica et al., 2001; Lambeck et al., 2017). This process can have a significant effect on local sea level near the location of change of continental water source (J. Sun et al., 2022). Second, water added or taken from the oceans moves the centre of mass of the Earth and is redistributed on a rotating Earth accord-

ing to particular spatial patterns (Mitrovica et al., 2001; Tamisiea et al., 2010) and affects sea level in the far-field. Third, elastic deformation of the ocean floor occurs due to changing ocean mass loads (Mitrovica et al., 2001, 2011), affecting both near-field and far-field ocean heights. Sea level fingerprints (Tamisiea et al., 2010; Kim et al., 2019; J. Sun et al., 2022) can be used to calculate the spatial pattern of change of ocean height related to mass changes on land.

The Gravity Recovery and Climate Experiment (GRACE) and GRACE Follow-On (GRACE-FO) space gravity missions provide near-continuous data from 2002 to present from which estimates of change in mass distribution on Earth can be made (Tapley et al., 2004, 2019). The leakage of signals between continents and oceans has been problematic in the analysis of space gravity data when estimating changes in mass distribution using spherical harmonic basis functions (Chen et al., 2009; Velicogna & Wahr, 2006). Various re-scaling strategies have been invoked (Watkins et al., 2015; Wiese et al., 2016), as well as novel forward modelling approaches to re-instate leaked signal back to the likely correct location on the continents (Chen et al., 2009; Jeon et al., 2021). The use of mass concentration elements (mascons) (Mueller & Sjogren, 1968), rather than spherical harmonics, helps to reduce the leakage of signal by permitting more direct spatial constraints on parameters to be applied (Rowlands et al., 2005; Watkins et al., 2015; Tregoning et al., 2022). Irregular-shaped mascons, that follow coastlines with an accuracy of <9 km, further reduce the leakage of signal between continents and oceans (Tregoning et al., 2022).

Through the use of forward modelling of GRACE estimates of terrestrial water storage change and sea level fingerprints, agreement was found between regional ocean height changes and those observed by satellite altimetry (Jeon et al., 2021). A similar forward-modelling approach was used to estimate a 0.32 mm/yr terrestrial water storage contribution to global sea level, leading to a tighter closure of the total sea level budget (Kim et al., 2019). Contributions to global sea level by each continent (plus Greenland and Antarctica) have been assessed in the literature (Rodell et al., 2019).

Separating the contributions from ice-covered regions and the rest of the continental land areas permits a more detailed assessment of how continental hydrological processes affect the spatial pattern of sea level height change. The latter includes ground-water variations, impounding of water in dams and reservoirs, and changes in soil moisture volumes. We quantify the integrated change of these components, or total water storage (TWS), from an analysis of GRACE/GRACE-FO measurements. We then convolve these mass changes with sea level fingerprints to construct time series of regional ocean mass change, caused by continental hydrology (i.e. excluding ice-based mass changes) to identify the continental hydrology sources of changes in local sea level at certain locations.

## 2 Space gravity data analysis

We estimate changes in mass on Earth as a change in height of a water column on 12,755 irregularly shaped mascons using the range acceleration as the key inter-satellite observation of the GRACE and GRACE Follow-On space gravity missions (Allgeyer et al., 2022). Data from August 2002 to September 2023 were processed, using the hybrid ACH1B data to model the non-gravitational accelerations on the GRACE-D satellite (Harvey et al., 2022). Non-linear effects in accelerometer measurements, caused by thermal variations within the satellites, were mitigated using a high-pass filtering approach (McGirr et al., 2022). This enables the number of accelerometer calibration parameters to be limited to one bias and one scale per day per orthogonal axis for the GRACE data and for GRACE-FO data up to the end of 2022. We computed degree-1 contributions from a combination of GRACE and ocean model data (Y. Sun et al., 2016) and the  $C_{2,0}$  estimates were replaced with values derived from satellite ranging data (Loomis et al., 2020). The values of  $C_{3,0}$  were also replaced for the GRACE-FO data. We formed normal equa-

tions for 24-hour orbital arcs, then stacked these daily normal equations to form monthly solutions, defined using calendar months.

We regularise the solutions to overcome the noise inherent in inversions of space gravity data, applying the same values to mascons using broad spatial regions. The off-diagonal elements of our regularisation matrix are zero and the diagonal elements are  $1/\sigma^2$  as shown in Figure S1. The regularisation matrix is applied for each day included in the monthly solution and we use the same regularisation for each monthly solution to keep the analysis process as generic as possible.

### 3 Calculation of sea level fingerprints

For a 1 m change in water storage on each land mascon, we calculated the corresponding change in water height of each ocean mascon (the code used for this calculation is that employed by Lambeck et al. (2017)). We include in the computations the rotational, gravitational and elastic deformation signals caused by the mass exchange between land and oceans. The computations are done on a radially symmetric, spheroidal elastic Earth using the elastic structure of the PREM model (Dziewonski & Anderson, 1981). Visco-elastic effects are insignificant and have not been included because the magnitudes of load variations are small ( $<15$  m) and the time scale of the variations is short ( $<1$  month). The monthly mass changes on land are multiplied by the computed fingerprints to apportion the signals over the oceans, thus deriving corresponding monthly ocean signals.

## 4 Results

### 4.1 Terrestrial water storage contributions to sea level

We are interested in the ocean mass changes from continental hydrology signals. To isolate these signals from ice-related signals over continents, we excluded mass changes over Greenland, Antarctica, the Alaskan and Patagonian glaciers as well as the ice-covered regions of Northeast Canada (Baffin Island, Ellesmere Island), Svalbard and Russian Arctic islands (Severnaya Zemlya and Novaya Zemlya). We calculated separately the ocean mass changes caused by these excluded regions.

Continental hydrology signals in ice-free regions (grey areas; Figure 1a) contribute 23% to the global ocean mass budget, with the remaining portion (77%) accounted for by melting mountain glaciers and ice-sheets which are predominantly found at high latitudes (grey areas; Figure 1b). Although the contribution of ice-covered regions to global mean sea level is  $\sim 3$ -times greater than ice-free regions, these continental hydrology signals contribute significantly to regional rates of sea level change. The rate of ocean mass increase from continental hydrology over the GRACE and GRACE-FO era has a distinct spatial pattern driven predominantly by total water storage (TWS) trends in Asia (Figure 1a). Meanwhile, the spatial pattern of the sea level fingerprint due to ice-melt causes near-uniform sea-level rise in mid-to-low latitude areas (Figure 1b). The fingerprint of continental hydrology contributions to sea-level results in both the mitigation or amplification of ocean mass increase due to melting ice at different locations (Figure S2).

Declining TWS in Asia over the GRACE and GRACE-FO era has led to an increase of up to 0.8 mm/yr around Africa, across the central Atlantic Ocean, around Australia and surrounding Pacific Island nations and in the North Pacific Ocean. The significant reductions in continental hydrology contributions of ocean mass in the Black Sea, eastern Mediterranean Sea and the Persian Gulf are caused by decreased strength in the direct gravitational attraction due to declining TWS in Asia since 2002, including around -0.1 mm/yr due to decreased water storage in the Caspian Sea. Although typically less than 1 mm/yr, local ocean mass changes driven by continental hydrology are compara-

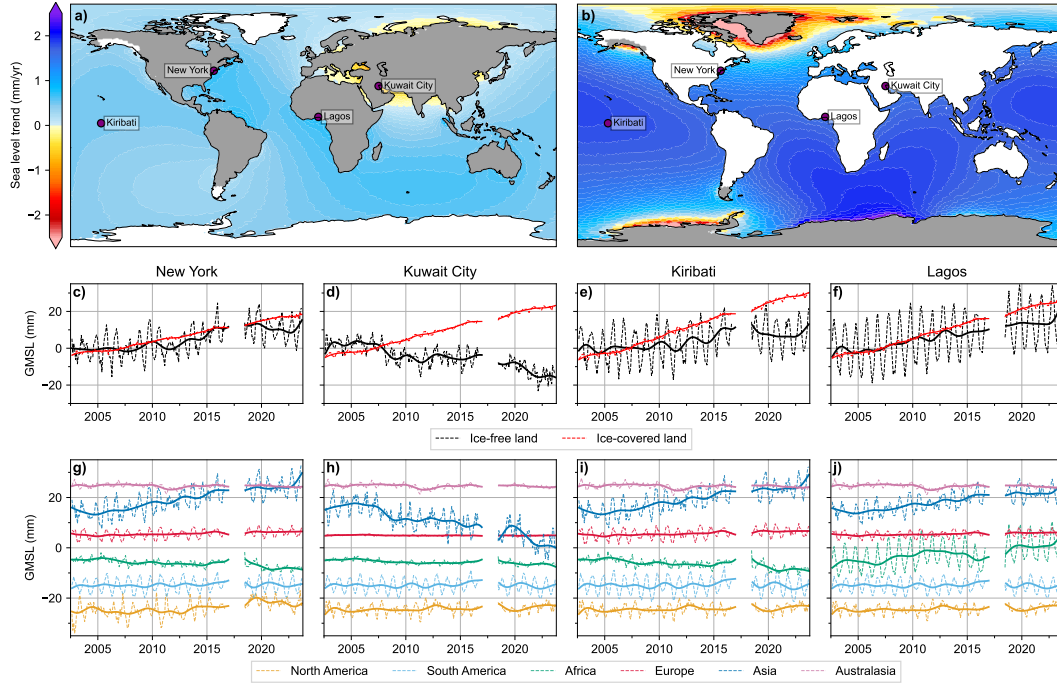


**Figure 1.** Rate of ocean mass change due to (a) continental hydrological processes, excluding ice-related signals (b) ice-covered regions. Mascons used to compute the ocean signals from continental hydrology in specific regions are indicated (grey). (c-f) time series of global mean sea level (GMSL) changes at sites indicated in a) from ice- and continental-related ocean contributions. Monthly values (dashed lines) and low-pass filtered values (solid) are plotted. (g-j) Contributions of six continental regions (as defined in Figure S3) to the changes in ocean mass at each location (each time series is offset by 10 mm).

ble to or greater than individual contributions of the Greenland (+0.77 mm/yr) and Antarctic (+0.33 mm/yr) ice sheets over the past two decades (Rodell et al., 2019; Tapley et al., 2019).

## 4.2 Local sea level changes

The spatial variability of the contributions of both ice-based and continent hydrology to ocean mass change creates a complex pattern from which to extract a comprehensive synthesis of local information. We focus on particular locations where the magnitudes of rates of continental hydrology contributions are high.

The largest increase in ocean mass caused by continental hydrology occurs around the coast of the Gulf of Guinea, central-west Africa near Lagos (Figure 1a). The increase in total ocean mass during the GRACE period near Lagos amounts to  $\sim 18$  mm of which 36% is derived from contributions from continental hydrology (Figure 1f). Similarly, along the east coast of North America, the magnitude of ice- and continent-based contributions is comparable from 2002-2019, at  $\sim 13$  mm, as seen in the time series for New York (Figure 1c). Interestingly, the decline at New York of sea level change contributions from continental hydrology after 2020 occurs because of the reduced contributions from Asia and increased wetting of the African continent drawing more water from the oceans (Figure 1g).

In contrast, the total ocean mass change at Kuwait City in the western Persian Gulf is only  $\sim 12$  mm over the 2002-2023 period. Here, the increase due to ice-based contributions (+29 mm) is compensated by  $>50\%$  due to continental hydrology contributions (-17 mm) (Figure 1d). The significant negative ocean mass signal here is driven by contributions from Asia (dark blue line in Figure 1h), including a  $\sim 2$  mm reduction of direct attraction by 2023 because of water loss in the Caspian Sea. Changes in TWS in Europe have virtually no impact on sea level in the Persian Gulf (purple line in Figure 1h).

Continental hydrology trends are  $\sim 0.5$  mm/yr throughout the Pacific island nations and ice-based contributions typically contribute 70-80% of the overall ocean mass increase. During the study period, Kiribati, located in the southwest Pacific Ocean, has experienced a total ocean mass increase of 48 mm, of which 10 mm are contributed by non-ice hydrological processes (Figure 1e). Kiribati has experienced a higher proportion of ocean mass increase driven by ice mass loss compared to most other Pacific Island nations.

### 4.3 The 2019-2023 triple La Niña

During the GRACE/GRACE-FO period the El Niño Southern Oscillation (ENSO) index was mostly in its strong negative phase ( $>-0.5$ ) from mid-2010 to early 2012 and again from late 2020 through to early 2023, resulting in the 2010/2011 strong La Niña and three consecutive years of La Niña conditions from 2020-2023 (Figure 2). La Niña brings significantly increased rainfall to large portions of Northern South America and the Australian landmass (Holgate et al., 2022). These two extended periods of La Niña conditions resulted in record flooding across the eastern seaboard of Australia (Fryirs et al., 2023).

The earlier La Niña event of 2010/2011 caused a drop in global sea level of several millimetres as ENSO conditions transitioned from a strong El Niño event to a strong La Niña event during 2010 (Boening et al., 2012). The associated decrease in ocean mass during 2010 is visible in the GRACE record and altimetric measurements of sea surface height corrected for steric expansion of the ocean (Figure 2e). During the two-year period, ocean height reductions of  $-0.9$  mm/yr and  $-0.82$  mm/yr were caused by increased TWS in northern South America and Australia, respectively (Figure 2a,b). In contrast, 2020-2023 saw sustained but comparatively weak La Niña conditions which caused a reduction in the rate of ocean mass increase over the three-year period. The recent triple La Niña resulted in a more modest contribution from Australia and northern South America to ocean mass of  $0.25$  mm/yr and  $0.76$  mm/yr, respectively. The total ocean mass measured by GRACE-FO exhibits a reduced rate of increase over this three-year period (Figure 2e). ENSO transitioned from a strong El Niño to neutral to weak La Niña conditions during the GRACE and GRACE-FO mission gap, this period corresponds to a 2-year interruption in the increase in ocean mass measured by steric-corrected altimetry (Figure 2e).

The consecutive La Niña events of 2010-2012 and 2020-2023 removed a total  $\sim 3.44$  mm and  $\sim 3.1$  mm of water from the oceans, and deposited it onto the Australian and northern South American landmasses over the two-year and three-year periods, respectively. These rates of TWS gain are comparable to the longer-term contributions of the polar ice sheets to the global ocean ( $+0.33$  mm/yr for Antarctica,  $+0.77$  mm/yr for Greenland) (Rodell et al., 2019)

Similar spatial patterns of change in ocean mass occurred during the two periods of consecutive La Niña events that occurred during GRACE and GRACE-FO mission operation (Figure 2c,d). However, the triple La Niña ocean increase is more localised off eastern Australia and the negative ocean mass signals in the far-field oceans are approximately double the magnitude in the earlier event. The increase in ocean mass around



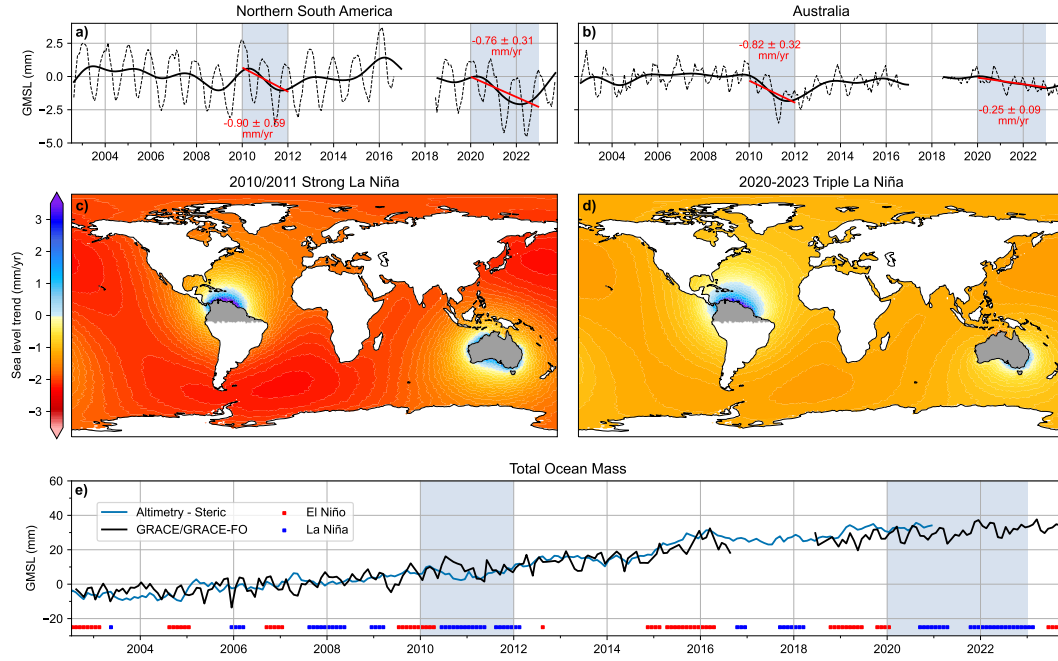


**Figure 2.** Change in terrestrial water storage integrated over a) northern South America, and b) the Australian continent in terms of global mean sea level (GMSL). Rate of ocean mass change derived using sea level fingerprints to apportion over the oceans the rate of change of TWS for each Australian mascon over c) the 2010-2011 La Niña event, and d) the triple La Niña period (2020-2023). GMSL from total ocean mass change measured by GRACE and GRACE-FO (black) and barystatic sea level changes from steric-corrected (blue)(Barnoud et al., 2023). The red and blue bars indicate the occurrence of El Niño and La Niña events, respectively (, )

the coastline of Australia and northern South America during La Niña periods is due to the stronger direct gravitational attraction of the ocean to the increased water mass on each continent (Figure 2c,d). The southern Atlantic and northern Pacific Oceans lost water during the La Niña precipitation events in Australia.

#### 4.4 Anthropogenic impacts on sea level

The combination of sea-level fingerprints and estimates of TWS changes allows the direct attribution of sea-level changes to natural climate variability and anthropogenic impacts on water storage contributions. The growing demand for water resources due to socioeconomic development and population growth has resulted in the depletion of groundwater resources in areas such as northern India and the North China Plain. Groundwater extraction in northern India (Rodell et al., 2009, 2019) is ongoing at a rate of 18 Gt/yr (equivalent to +0.05 mm/yr global sea level) during the past two decades (Figure 3a), causing a 1 mm increase in global sea level from 2002 to 2023. However, the rate of TWS decline in northern India during the GRACE-FO era is significantly slower at +0.02 mm/yr global sea level. Annual precipitation has not increased significantly during this time, suggesting that rates of groundwater abstraction have slowed since 2018 (Figure 3a).

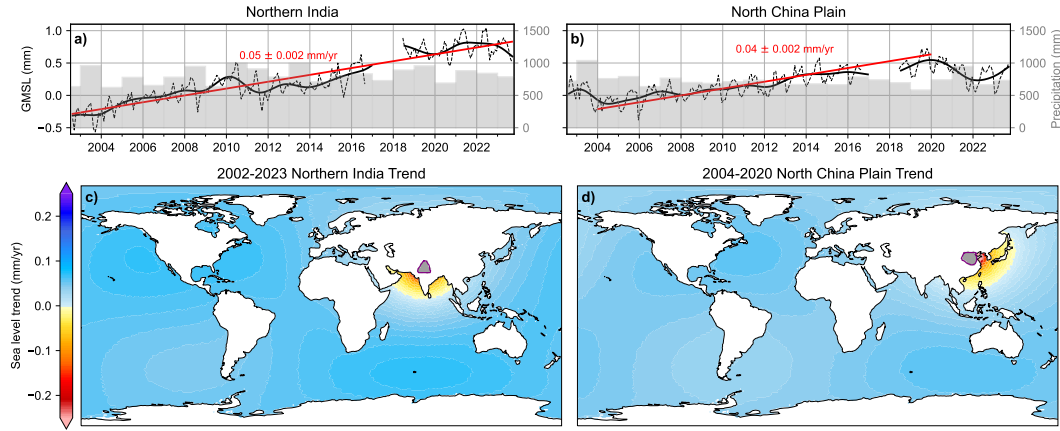


**Figure 3.** Time series of changes in TWS (black dashed line), low-pass filtered TWS (black solid line) and 2002-2023 and 2004-2020 TWS trends for a) northern India, and b) North China Plain, respectively, in mm of Global Mean Sea Level (GMSL). Corresponding rates of ocean mass change derived using sea level fingerprints to apportion each of these anthropogenic signals over the oceans (c,d). Mascons used to compute the ocean signals from continental hydrology in specific regions are indicated (grey). Grey bars indicate total annual precipitation in mm calculated from ERA5 monthly reanalysis (, ).

Following a record year of precipitation in 2003, TWS in the North China Plain declines, contributing  $+0.04$  mm/yr to global mean sea level until 2020 (Figure 3b). The contribution of North China Plain TWS to global sea level reverses during the GRACE-FO era, storing  $0.05$  mm/yr of global mean sea level on the continent. This reversal in trend is likely due to the combined effect of significant increases in precipitation in 2021 (Figure 3b) and decreased groundwater abstraction due to the implementation of policies to reduce irrigation and south to north water diversion, resulting in groundwater recharge over GRACE-FO period (Long et al., 2020; Zhang et al., 2022). Furthermore, the increase in TWS corresponds to a reduction in water use due to the slowdown in manufacturing during the Covid-19 pandemic (Shu et al., 2023) and recharge due to environmental flow releases since 2019 (Liu et al., 2023).

Groundwater extraction in northern India over the GRACE and GRACE-FO period have resulted in a fall in sea level, due to a reduction in the strength of the direct gravitational attraction of the ocean to continental water stores, of a maximum negative rate of  $-0.15$  mm/yr along the coastline of southern Pakistan (Figure 3c). Groundwater extraction in the North China Plain (Rodell et al., 2019) between 2004 and 2020 caused the sea level to fall in the East China Sea by up to  $-0.54$  mm/yr during this period due to the reduced gravitational attraction of the oceans to the China landmass (Figure 3d). This is almost a factor of  $\sim 4$  greater than the signal caused by groundwater extraction in India because the source is much closer to the ocean, despite a comparable contribution to global mean sea level. The peak increases in ocean mass due to the groundwater extraction in India (2002-2023) and China (2004-2020) occurred in the northwestern Atlantic and Southern Ocean, having the largest impact on sea level in North America and along the South Australian and South African Coastlines (Figure 3d).



## 5 Conclusion

Continental hydrological processes in regions that are not ice-covered have contributed to ocean mass increase on multi-decadal time-scales throughout the GRACE/GRACE-FO era. Although they contribute tens of millimetres to regional sea level in some instances, these impacts are not likely to persist indefinitely. For example, the Asian continent, which contributed to the increase in global ocean mass (2003-2020), has been drawing water from the oceans since 2020. Natural climate variability, such as La Niña events, affect sea level with rates comparable to present day contributions of the polar ice sheets, although these former effects tend to persist for only a few years. Anthropogenic intervention, such as extraction of groundwater resources, increases ocean mass in the far field, but causes decreases in local sea level of up to  $\sim 1$  mm/yr. These rates of near-field sea level fall are also comparable in magnitude to the longer-term contributions of the polar ice sheets and mountain glaciers, at times masking  $\sim 80\%$  of the sea level increase caused by melting of ice-covered regions. If this extraction of groundwater ceases, then near-field regions (such as the Persian Gulf, eastern Mediterranean, East China Sea, and coastline of southern Pakistan) would see an increase in the rate of local sea level rise of up to 1 mm/yr, significantly increasing the vulnerability of these regions to sea level rise. However, if current trends in groundwater abstraction remain, continental hydrology would continue to compound sea level rise caused by melting of continental ice in the far-field. Currently,  $>25\%$  of total sea level rise around Africa, across the central Atlantic Ocean, around Australia and surrounding Pacific Island nations, and in the North Pacific Ocean are due to the declining trend in Asia's terrestrial water storage between 2002 and 2023.

## 6 Open Research

The GRACE and GRACE Follow-On data are available from [podaac.jpl.nasa.gov/dataset](https://podaac.jpl.nasa.gov/dataset). The ANU mascon solution used in this analysis (ANU\_mascons\_RL02) is available in netcdf format at <https://datacommons.anu.edu.au/DataCommons/rest/display/anudc:6133> and can be visualised at <https://portal.auscope.org.au/>. The sea level fingerprints computed for our mascons are available at [add reference upon acceptance of manuscript]. Barystatic sea level changes were accessed at <https://doi.org/10.24400/527896/a01-2023.012>. Nino3.4 anomalies were accessed at [https://psl.noaa.gov/gcos\\_wgsp/Timeseries/Nino34/](https://psl.noaa.gov/gcos_wgsp/Timeseries/Nino34/). ERA5 monthly averaged reanalysis total precipitation was accessed at <https://cds.climate.copernicus.eu/cdsapp#!/dataset/reanalysis-era5-single-levels-monthly-means>.

## Acknowledgments

The analysis of the GRACE Follow-On data was funded in part through contracts with Geoscience Australia. R. McGirr was funded by the Australian Research Council Special Research Initiative, Australian Centre for Excellence in Antarctic Science (Project Number SR200100008).

## References

- Allgeyer, S., Tregoning, P., McQueen, H., McClusky, S., Potter, E.-K., Pfeffer, J., ... Montillet, J.-P. (2022). ANU GRACE data analysis: Orbit modeling, regularization and inter-satellite range acceleration observations. *Journal of Geophysical Research: Solid Earth*, 127(2), e2021JB022489. doi: <https://doi.org/10.1029/2021JB022489>
- Barnoud, A., Pfeffer, J., Cazenave, A., Fraudeau, R., Rousseau, V., & Ablain, M. (2023). Revisiting the global mean ocean mass budget over 2005–2020. *Ocean Science*, 19(2), 321–334.
- Boening, C., Willis, J. K., Landerer, F. W., Nerem, R. S., & Fasullo, J. (2012).

- 321 The 2011 La Niña: So strong, the oceans fell. *Geophysical Research Letters*,  
322 39(19).
- 323 Boyer, T., Domingues, C., Good, S., Johnson, G., Lyman, J., Ishii, M., ... Wijffels,  
324 S. (2016). Sensitivity of global ocean heat content estimates to mapping meth-  
325 ods, xbt bias corrections, and baseline climatology. *Journal of Climate*, 29.  
326 doi: <https://doi.org/10.1175/JCLI-D-15-0801.1>
- 327 Chen, J., Wilson, C., Blankenship, D., & Tapley, B. (2009). Accelerated Antarctic  
328 ice loss from satellite gravity measurements. *Nature Geoscience*, 2(12), 859–  
329 862. doi: <https://doi.org/10.1038/ngeo694>
- 330 Ciraci, E., Velicogna, I., & Swenson, S. (2019). Continuity of the mass loss of the  
331 world’s glaciers and ice caps from the GRACE and GRACE follow-on missions.  
332 *Geophys. Res. Lett.*. doi: <https://doi.org/10.1029/2019GL086926>
- 333 Dziewonski, A., & Anderson, D. (1981). Preliminary reference earth model. *Phys.*  
334 *Earth. Planet. Int.*, 25(4). doi: [https://doi.org/10.1016/0031-9201\(81\)90046-7](https://doi.org/10.1016/0031-9201(81)90046-7)
- 335 Fryirs, K., Zhang, N., Ralph, T. J., & Arash, A. M. (2023). Natural flood man-  
336 agement: Lessons and opportunities from the catastrophic 2023-2022 floods in  
337 eastern australia. *Earth Surface Processes and Landforms*, 48(9), 1649-1664.  
338 doi: <https://doi.org/10.1002/esp.5647>
- 339 Harvey, N., McCullough, C., & Save, H. (2022). Modeling grace-fo accelerometer  
340 data for the version 04 release. *Advances in Space Research*, 69(3), 1393-1407.
- 341 Holgate, C., Evans, J. P., Taschetto, A. S., Gupta, S., & Santoso, A. (2022). The  
342 impact of interacting climate modes on east australian precipitation mois-  
343 ture sources. *Journal of Climate*, 3147-3159. doi: <https://doi.org/10.1175/JCLI-D-21-0750.1>
- 344 Jeon, T., Seo, K.-W., Kim, B.-H., Kim, J.-S., Chen, J., & Wilson, C. R. (2021). Sea  
345 level fingerprints and regional sea level change. *earth and Planetary Science*  
346 *Letters*, 567(116985). doi: <https://doi.org/10.1016/j.epsl.2021.116985>
- 347 Kim, J.-S., Seo, K.-W., Jeon, T., Chen, J., & Wilson, C. R. (2019). Missing hy-  
348 drological contribution to sea level rise. *Geophys. Res. Lett.*. doi: 10.1029/  
349 2019GL085470
- 350 Lambeck, K., A., P., & Zhao, S. (2017). The north american late wisconsin ice sheet  
351 and mantle viscosity from rebound analyses. *Quat. Sci. Rev.*, 158, 172-210.
- 352 Leblanc, M. J., Tregoning, P., Ramillien, G., Tweed, S. O., & Fakes, A. (2009).  
353 Basin-scale, integrated observations of the early 21st century multiyear  
354 drought in southeast Australia. *Water Resources Research*, 45(4).
- 355 Liu, S., Zhou, Y., McClain, M. E., & Wang, X. (2023). Effects of downstream en-  
356 vironmental flow release on enhancing the groundwater recharge and restoring  
357 the groundwater/surface-water connectivity in Yongding River, Beiging, China.  
358 *Hydrogeology Journal*. doi: <https://doi.org/10.1007/s10040-023-02675-w>
- 359 Long, D., Yang, W., Scanlon, B. R., Zhao, J., Liu, D., Burek, P., ... Wada, Y.  
360 (2020). South-to-North Water Diversion stabilizing Beijing’s groundwater  
361 levels. *Nature Communications*, 11(1), 3665.
- 362 Loomis, B. D., Rachlin, K. E., Wiese, D. N., Landerer, F. W., & Luthcke, S. B.  
363 (2020). Replacing GRACE/GRACE-FO C<sub>30</sub> with satellite laser ranging: Im-  
364 pacts on Antarctic ice sheet mass change. *Geophysical Research Letters*, 47(3),  
365 e2019GL085488. doi: <https://doi.org/10.1029/2019GL085488>
- 366 McGirr, R., Tregoning, P., Allgeyer, S., McQueen, H., & Purcell, A. (2022). Mit-  
367 igation of thermal noise in GRACE accelerometer observations. *Advances in*  
368 *Space Research*, 69(1), 386-401.
- 369 Mitrovica, J., Gomez, N., Morrow, E., Hay, C., Latychev, K., & Tamisiea, M.  
370 (2011). On the robustness of predictions of sea level fingerprints. *Geophys.*  
371 *Res. Int.*, 187(2), 729-742.
- 372 Mitrovica, J., Tamisiea, M., Davis, J., & Milne, G. (2001). Polar ice mass variations  
373 and the geometry of global sea level change. *Rev. Geophys.*, 409, 1026-1029.
- 374 Mueller, P., & Sjogren, W. L. (1968). Mascons: Lunar mass concentrations. *Science*,  
375

161. doi: <https://doi.org/10.1126/science.161.3842.680>
- Rodell, M., Famiglietti, J. S., Wiese, D. N., Reager, J. T., Beaulieu, H. K., Landerer, F. W., & Lo, M.-H. (2019). Emerging trends in global freshwater availability. *Nature*, 557. doi: <https://doi.org/10.1038/s41586-018-0123-1>
- Rodell, M., Velicogna, I., & Famiglietti, J. S. (2009). Satellite-based estimates of groundwater depletion in India. *Nature*, 460(7258), 999–1002.
- Roemmich, D., Johnson, G., Riser, S., Davis, R., Gilson, J., Brechner Owens, W., ... Ignaszewski, M. (2009). The argo program: Observing the global ocean with profiling floats. *Oceanography*, 22. doi: <https://doi.org/10.5670/oceanog.2009.36>
- Rowlands, D., Luthcke, S., Klosko, S., Lemoine, F. G., Chinn, D., McCarthy, J., ... Anderson, O. (2005). Resolving mass flux at high spatial and temporal resolution using GRACE intersatellite measurements. *Geophysical Research Letters*, 32(4). doi: <https://doi.org/10.1029/2004GL021908>
- Shu, F., Lui, H., Fu, G., Sun, S., Li, Y., Ding, W., ... Zhang, L. (2023). Unraveling the impact of covid-19 pandemic dynamics on commercial water-use variation. *Journal of Water Resources Planning and Management*, 149(8). doi: <https://doi.org/10.1061/JWRMD5.WRENG-5940>
- Sun, J., Wang, L., Peng, Z., Fu, Z., & Chen, C. (2022). The sea level fingerprints of global terrestrial water storage changes detected by grace and grace-fo data. *Pure and Applied Geophysics*. doi: <https://doi.org/10.1007/s00024-022-03123-8>
- Sun, Y., Riva, R., & Ditmar, P. (2016). Optimizing estimates of annual variations and trends in geocenter motion and  $j_2$  from a combination of grace data and geophysical models. *Journal of Geophysical Research*. doi: <https://doi.org/10.1002/2016JB013073>
- Tamisiea, M. E., Hill, E. M., Ponte, R. M., Davis, J. L., Velicogna, I., & Vinogradova, N. T. (2010). Impact of self-attraction and loading on the annual sea level cycle. *Journal of Geophysical Research*, 115(C07004). doi: <https://doi.org/10.1029/2009JC005687>
- Tapley, B. D., Bettadpur, S., Watkins, M., & Reigber, C. (2004). The gravity recovery and climate experiment: Mission overview and early results. *Geophysical Research Letters*, 31(9). doi: <https://doi.org/10.1029/2004GL019920>
- Tapley, B. D., Watkins, M. M., Flechtner, F., Reigber, C., Bettadpur, S., Rodell, M., ... others (2019). Contributions of GRACE to understanding climate change. *Nature climate change*, 9(5), 358–369. doi: <https://doi.org/10.1038/s41558-019-0456-2>
- Tregoning, P., McGirr, R., Pfeffer, J., Purcell, A., McQueen, H., Allgeyer, S., & McClusky, S. (2022). ANU GRACE data analysis: Characteristics and benefits of using irregularly shaped mascons. *Journal of Geophysical Research: Solid Earth*, 127(2), e2021JB022412. doi: <https://doi.org/10.1029/2021JB022412>
- Velicogna, I., & Wahr, J. (2006). Measurements of time-variable gravity show mass loss in Antarctica. *Science*, 311(5768), 1754–1756. doi: <https://doi.org/10.1126/science.1123785>
- Velicogna, I., & Wahr, J. (2013). Time-variable gravity observations of ice sheet mass balance: Precision and limitations of the GRACE satellite data. *Geophys. Res. Lett.*, 40, 3055–3063.
- Watkins, M. M., Wiese, D. N., Yuan, D.-N., Boening, C., & Landerer, F. W. (2015). Improved methods for observing Earth’s time variable mass distribution with GRACE using spherical cap mascons. *Journal of Geophysical Research: Solid Earth*, 120(4), 2648–2671. doi: <https://doi.org/10.1002/2014JB011547>
- Wiese, D. N., Landerer, F. W., & Watkins, M. M. (2016). Quantifying and reducing leakage errors in the JPL RL05M GRACE mascon solution. *Water Resources Research*, 52(9), 7490–7502. doi: <https://doi.org/10.1002/2016WR019344>
- Wouters, B., S., G. A., & Moholdt, G. (2019). Global glacier mass loss during the

431 GRACE satellite mission (2002-2016). *Front. earth Sci.*, 7. doi: [https://doi](https://doi.org/10.3389/feart.2019.00096)  
432 [.org/10.3389/feart.2019.00096](https://doi.org/10.3389/feart.2019.00096)  
433 Zhang, Y., Zhou, W., Wang, X., Chen, S., Chen, J., & Li, S. (2022). Indian ocean  
434 dipole and ENSO's mechanistic importance in modulating the ensuing-summer  
435 precipitation over eastern china'. *Climate and Atmospheric Science*, 48. doi:  
436 <https://doi.org/10.3389/feart.2019.00096>